MONTHLY NOTICES of the Royal Astronomical Society

Core and conal component analysis of Pulsar B1237+25 --- II. Investigation of the Segregated Modes

Journal:	*Monthly Notices of the Royal Astronomical Society*
Manuscript ID:	MN-13-0973-MJ.R1
Manuscript type:	Main Journal
Date Submitted by the Author:	n/a
Complete List of Authors:	Rankin, Joanna; University of Vermont, Physics Smith, Emily; University of Vermont, Physics Mitra, Dipanjan; National centre for Radio Astrophysics, TIFR, Astrophysics
Keywords:	(stars:) pulsars: general < Stars, (stars:) pulsars: individual:... < Stars, techniques: polarimetric < Astronomical instrumentation, methods, and techniques, methods: analytical < Astronomical instrumentation, methods, and techniques, radiation mechanisms: non-thermal < Physical Data and Processes, polarization < Physical Data and Processes

Mon. Not. R. Astron. Soc. **000**, 1–?? (year) Printed 21 June 2013 (MN LATEX style file v2.2)

Core and Conal Component Analysis of Pulsar B1237+25 — II. Investigation of the Segregated Modes

Emily Smith[1], Joanna Rankin[1,2] & Dipanjan Mitra[3]
[1]*Physics Department, University of Vermont, Burlington, VT 05405*⋆
[2]*Sterrenkundig Instituut 'Anton Pannekoek', University of Amsterdam, NL-1090 GE*
[3]*National Centre for Radio Astrophysics, Ganeshkhind, Pune 411 007 India*†

In original form year month day

ABSTRACT

Radio pulsar B1237+25 is the prime exemplar of a five-component profile indicating a core/double cone emission-beam structure, and here we conduct a pulse-sequence analysis of its three distinct behaviours based on the partial profile study published earlier as Paper I. The core region has demanded most of our attention, and we have found first that the two "orthogonal" polarization modes (OPMs) are far from orthogonal in this region and second that aberration/retardation (A/R) of the secondary OPM is responsible. We found this A/R effect as expected both in the retarded core power and the delayed polarization-position angle (PPA) signature. In these terms the A/R effect seems to reflect a cascade or linear amplifying process along the magnetic axis extending to a height of some 230 km—indeed, very similar to what was found earlier for pulsar B0329+54.

The pulsar's three contrasting "states" reflect different conditions of core activity: in the quiet normal mode, core emission is barely perceptible, and the two cones exhibit phase-locked modulation in the manner of a rotating carousel beam system. In the flare-normal mode, this modulation persists for short intervals, but the core is more active, and it exhibits an intensity-dependent A/R associated **mainly with a single, apparently X, OPM/propagation** mode. Finally, the abnormal mode shows strong **continuous core emission—X trailing and O leading—that** appears to quench and distort the conal emission and its modulation. Again, the core radiation shows a strong intensity-dependent, **X-mode A/R, and the conal O-mode emission** also seems to be thrown forward from the trailing to the leading side of the profile relative to its normal mode configurations.

Key words: – pulsars: B1237+25, non-thermal radiation mechanisms

DEDICATION

This paper is dedicated to the memory of our colleague, Professor Donald C. Backer of the University of California at Berkeley, who pioneered research into drifting, nulling and moding, importantly through study of this very pulsar.

1 INTRODUCTION

The widely studied pulsar B1237+25 exhibits five components produced by a near-central traverse of the sight line through the emission region (Rankin 1993a,b; hereafter ET VI); see Figure 1. The five components[1] of the

⋆ emsmith424@gmail.com; Joanna.Rankin@uvm.edu
† dmitra@ncra.tifr.res.in

[1] We follow convention in numbering its leading outer, inner, core, and trailing inner and outer components 1-5, respectively.

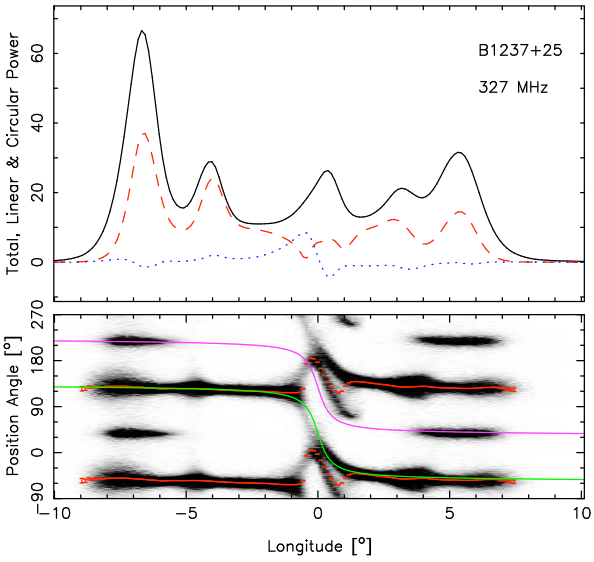

Figure 1. Total polarized profile of the 5209-pulse B1237+25 observation from 2005 January 8. Its relatively bright central core feature reflects the unusually strong contribution of abnormal mode apparitions in this observation. The edges are slightly truncated to better show details under the pulsar's core and two conal component pairs. The top panel gives the the total intensity (Stokes I; solid curve), the total linear (L ($=\sqrt{Q^2+U^2}$); dashed red), and the circular polarization (Stokes V; dotted blue). The PPA [$=\frac{1}{2\tan^{-1}(U/Q)}$] histogram (lower panel) corresponds to those samples having errors smaller than 8°, and it is plotted twice for clarity with the average PPA traverse overplotted (red). **The green and magenta model curves are discussed in the text.** The origin is taken near the profile center as determined by the Stokes V inflection point. Note the two linear polarization minima framing the central core emission as well as the two parallel PPA traverses in the –1 to +1.5° longitude region.

pulsar's emission consist of two concentric emission cones and a central core beam. The pulsar also exhibits emission modes, frequent nulling, and a 2.7-rotation-period (hereafter P_1) subpulse modulation (Backer 1970a,b,c, 1973). Pulsar B1237+25's rich phenomenology has been studied extensively; however, links between these effects and the appropriate physical emission mechanisms have not yet been clearly identified. In particular, since the publication of Paper I (Srostlik & Rankin 2005), we now understand a) that modes represent global changes in the magnetospheric "state" (*e.g.,* Kramer *et al.* 2006), b) that both nulls and *pseudo*nulls punctuate pulse sequences (*e.g.,* Herfindal & Rankin 2007, 2009) and c) that carousel action (Deshpande & Rankin 1999, 2001) not only underlies drifting subpulses but conal beams and other effects as well.

Traditionally, B1237+25 had been regarded as having two modes: its 'normal' and 'abnormal' modes (Backer 1970a,b,c, 1973). The 'normal' mode exhibited the classical double conal and weak core structure as well as a regular 2.7-P_1 subpulse modulation of its conal components (Bartel *et al.* 1982, hereafter BMSH; Hankins & Wright 1980). By contrast, the 'abnormal' mode is characterized by strong core emission, conflation of the trailing conal components, and cessation of the modulation. Additionally, each mode is distinguished by significant changes in both total power and polarization properties.

The presence of three modes was proposed in Paper I, rather than the traditional two identified by previous studies. The normal mode was found to have two distinguishable patterns of emission. Pulse sequences (hereafter PSs) with significant core emission were seen to interrupt mainly conal intervals regularly. In addition, these intervals of core activity differed in both polarization and total power. These distinctions prompted Srostlik & Rankin to divide the normal mode into a core-active 'flare-normal' mode and the core-weak 'quiet-normal' mode.

The three emission modes were suggested in part to better segregate and exhibit their particular orthogonal polarization modal (hereafter OPM) behaviours. The presence of OPM emission was identifiable both in modal partial average profiles and in the polarization characteristics of PSs. In particular, Paper I noted that the total average profile conflates all three modes, so the expected central 180°-polarization-position-angle (hereafter PPA) sweep **is distorted**. However, when a partial profile is constructed with pulses having little to no core emission, the PPA traverse is unusually abrupt and complete. This appeared to show that the total profile was comprised of both OPMs near the center under the core component.

As discussed by Rankin & Ramachandran (2003; hereafter ET VII), the depolarized edges of pulsar profiles also indicate the presence of OPM emission. This led to the conclusion that one OPM's emission is offset from the other in both magnetic colatitude and azimuth. The orthogonal polarization modes likely result from propagation effects as the waves pass through the dense magnetosphere. Various mechanisms for the production of pulsar OPM emission have been suggested [*e.g.,* Melrose (1979); Allan & Melrose (1982); Arons/Barnard 1986a,b]. Primarily, it seems that the emission $\parallel$ and $\perp$ to the projected magnetic field direction separate due to different refractive properties.

Therefore, in our analysis below, we explicitly assume that all pulsar radio emission escapes the magnetosphere oriented either $\parallel$ and $\perp$ to the projected magnetic field direction. The height at which this polarization is fixed may vary in different regions within the polar flux tube, but to the extent that the field is dipolar, the field orientation can be traced across the profile. Because EM-wave propagation is so constrained by the intense magnetic field to these two orientations, we can say little about the underlying emission physics on the basis of modal polarization.

In what follows, §2 describes our observations. §3 undertakes a nulling analysis, and §4 the respective emis-

sion modes. In §5 we discuss connections to the O and X propagation modes, §6 describes the OPM segregation analysis and §7 **studies of the different intensity levels (hereafter intensity fractions) of the various modes.** §8 reviews the dynamics of core emission, §9 then provides an analytical summary, and §10 a discussion of our results.

2 OBSERVATION

The observation used in our analyses was made using the 305-m Arecibo Telescope in Puerto Rico. The primary 327-MHz polarized PS was acquired using the upgraded instrument together with the Wideband Arecibo Pulsar Processor (WAPP) on 2005 January 8 comprised of 5209 pulses. The auto- and cross-correlation functions of the channel voltages produced by receivers connected to orthogonal linearly polarized feeds were three-level sampled. Upon Fourier transforming, 64 channels were synthesized across a 25-MHz bandpass with a 512-μs sampling time, providing a resolution of 0.133° **in pulse longitude and effectively swamping interstellar scintillation effects on a several hour timescale**. The Stokes parameters have been corrected for dispersion, interstellar Faraday rotation and various instrumental polarization effects. While most of the observation was of very high quality, a few percent of the pulses showed visible effects of interference, which complicated the mode segregation below. Errors in the PPA were computed relative to the off-pulse noise phasor—that is, $\sigma_{PPA} \sim tan^{-1}(\sigma_{off-pulse}/L)$.

3 NULLING ANALYSIS

Early study of B1237+25 observations had found that approximately 6% of its pulses were 'nulls' [reviewed in (Rankin 1986); hereafter ET III]. Using an appropriate threshold relative to the mean pulse intensity $< I >$ of 10%, our finding was similar. Additionally, Paper I identified a population of weak pulses that qualify as nulls, but exhibit appropriate polarization at particular longitudes which show them to be weak emission features.

By separating the total PS into normal and abnormal partial sequences, null histograms were computed to study the proportion of nulls or weak pulses within each mode; see Figure 2. The normal mode was thus found to have a null fraction of 5.2%, and this fraction was significantly larger than the 2.7% **for the abnormal mode**. This different nulling behaviour in the two modes is a new finding for B1237+25, but not surprising as several other pulsars are now **known to** exhibit a similar effect (*e.g.,* B2303+30; see Redman *et al.* 2005). In abnormal mode PSs, the greater intensity and prominent core emission may be related to the paucity of nulls. Those nulls that do occur are almost always single and bursts **(intervals of continuous emission between nulls)** of more

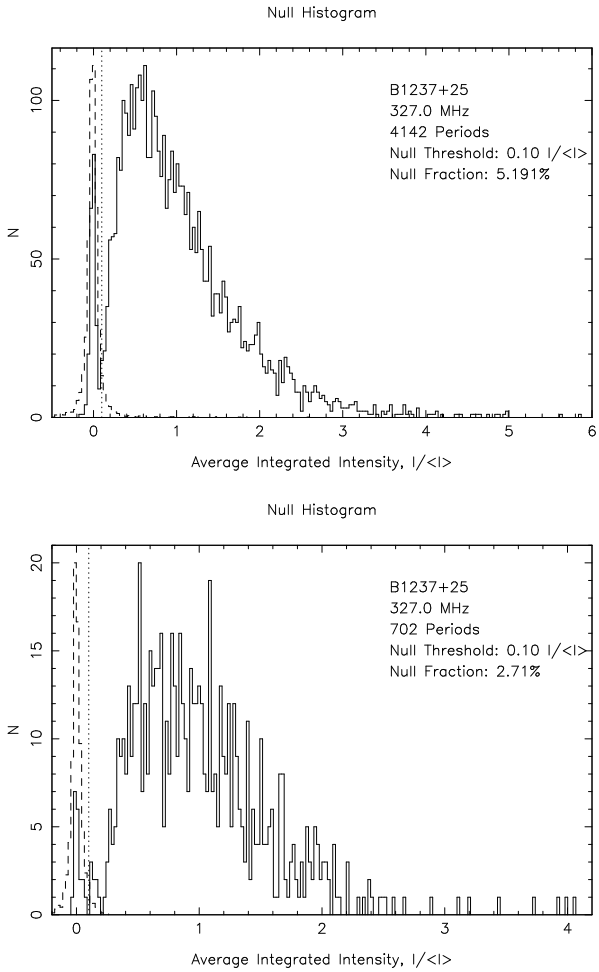

Figure 2. Histograms of Stokes I for the normal (upper) and abnormal (lower) modal PSs. The two partial PSs were 4142 and 702 pulses in length, respectively, **representing all the pulses that could be securely classified as one or the other of the two modes**. The nulls are segregated using a conservative threshold of $0.10 < I >$ indicated by the vertical dotted line.

than 20 pulses are favored; see Figure 3. In our 5209-pulse observation, which was relatively rich in abnormal mode intervals, only once or twice did a two-pulse null occur.

Normal mode nulls and bursts have a significantly different distribution. Not only are nulls more frequent at 5.2%, but nulls lasting for two or more pulses are far more common. Similarly, although many short bursts do occur, two having lengths of nearly 200 pulses occurred in our observations; see Figure 4. Here the Runs Test **(see Redman & Rankin 2009) then indicates that these nulls do not occur randomly—rather they are grouped such as to be highly** "undermixed" within normal mode PSs.

The weak emission features identified during many

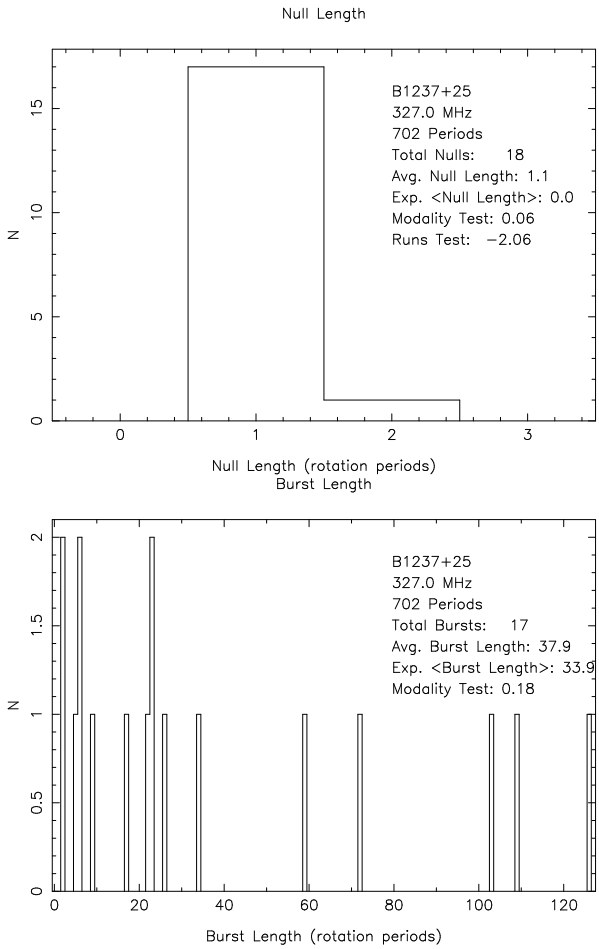

Figure 3. Null- and burst- length histograms as in Fig. 4 for the abnormal mode. Here single nulls are strongly favored and two-pulse nulls rare. Abnormal burst lengths of more than 20 pulses are favored, though some short bursts do occur.

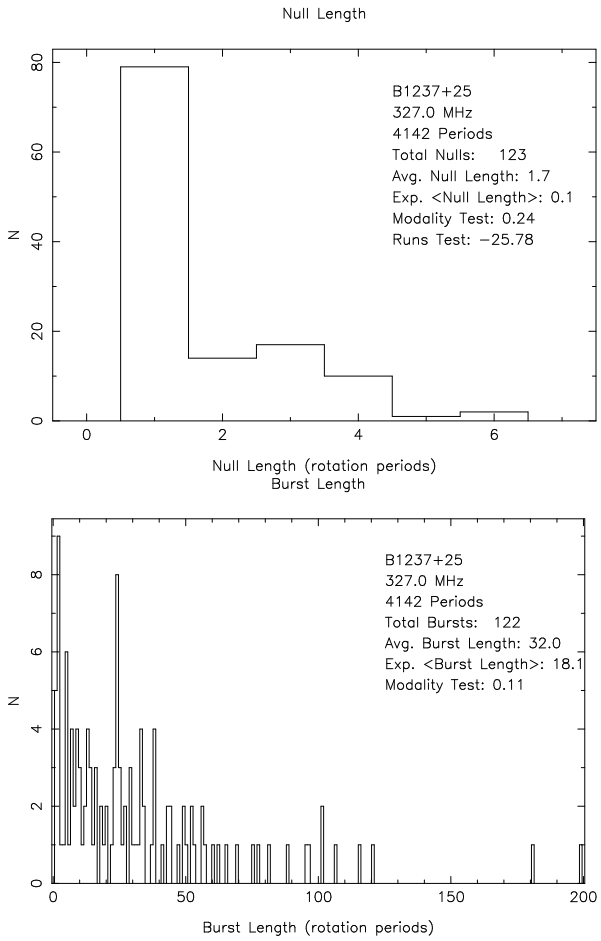

Figure 4. Null- and burst-length histograms for the normal mode. Null lengths of a single rotation are highly favored, however, long nulls of up to six pulses in length were found in our observation. Burst lengths ranged from a single pulse to intervals persisting for nearly 200 pulses.

of B1237+25's nulls in Paper I were noted in this observation as well. Many of the pulses, classified as nulls by failing the $0.10 < I >$ threshold—particularly those lasting for several pulses—had very discernible weak, highly polarized emission throughout the "null". This **"sputtering"** effect is similar to that found in B0818–13 by Janssen & van Leeuwen (2004) and suggests that these nulls are in fact *pseudo*nulls wherein there is no cessation of the pulsar's emission engine.

4 THE TWO OR THREE EMISSION MODES

Since the time of Don Backer's pioneering studies in the early 1970s, B1237+25 was regarded as having two distinct modes, the normal (N) and abnormal (Ab) modes. Paper I then argued that the N mode is comprised to two distinct behaviours, a core-active, flare-normal (FN) mode, and a weak core, quiet-normal (QN) mode. In what follows, we will treat both modal schemes in an effort to discern detailed aspects of the pulsar's emission characteristics.

Figure 5 (upper left) gives a normal (N) mode partial profile for the observation under study. Its 3907 constituent pulses were identified by inspecting each pulse of the full observation and segregating those pulses that exhibited the weak core, full profile normal mode characteristics as opposed to the strong core, curtailed profile properties of the abnormal (Ab) mode. Nulls were omitted. Note the overall larger fractional linear polarization, the clear OPM emission under the outer conal components, and the weak core feature with an even weaker hint of an anti-symmetric circularly polarized V signature. There is much to see as well in the PPA behaviour in the center of the profile. First, as discussed in Paper I, the average PPA traverse fails to exhibit the expected steep, nearly 180° traverse here, and that discussion ar-

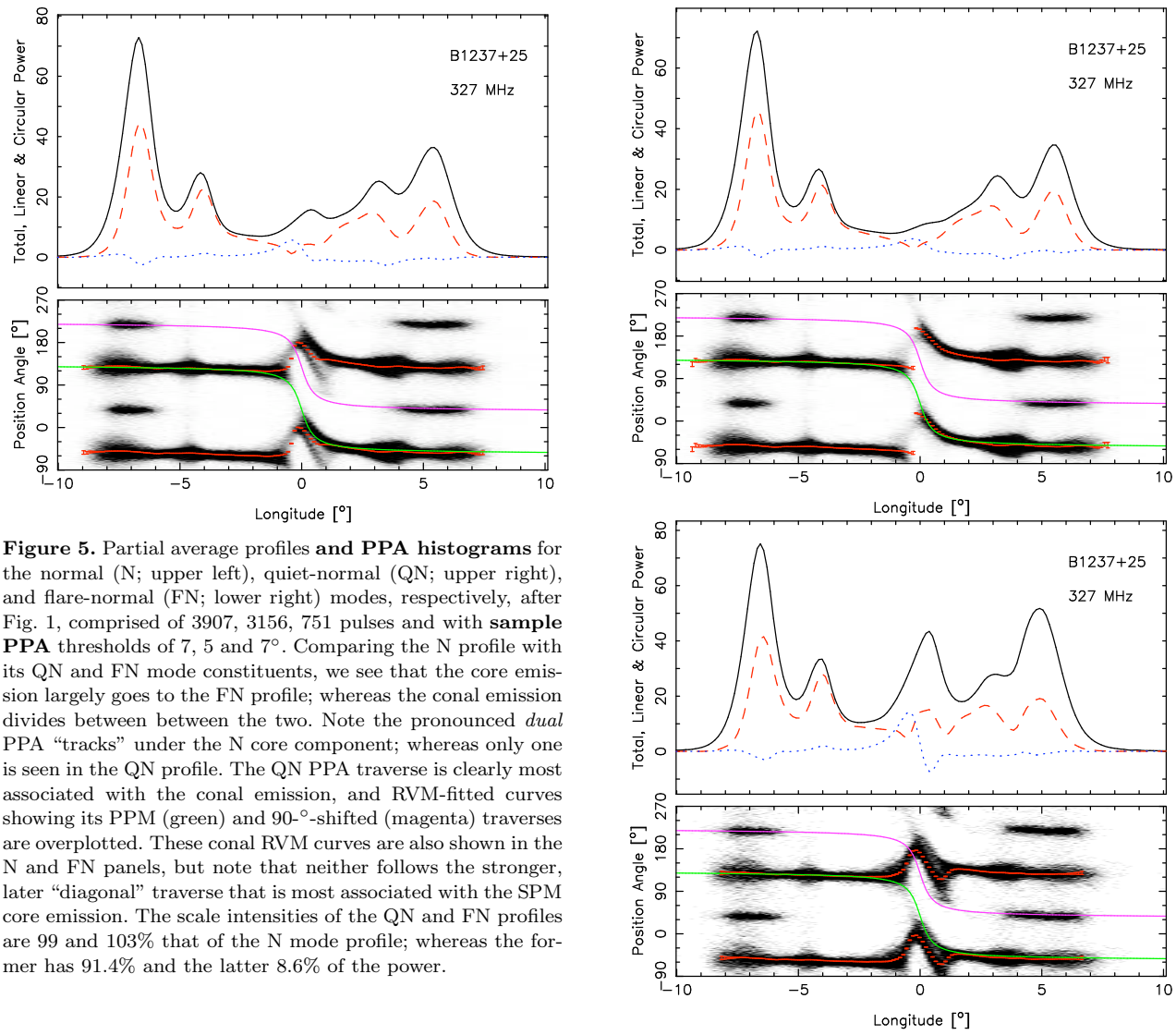

Figure 5. Partial average profiles **and PPA histograms** for the normal (N; upper left), quiet-normal (QN; upper right), and flare-normal (FN; lower right) modes, respectively, after Fig. 1, comprised of 3907, 3156, 751 pulses and with **sample PPA** thresholds of 7, 5 and 7°. Comparing the N profile with its QN and FN mode constituents, we see that the core emission largely goes to the FN profile; whereas the conal emission divides between between the two. Note the pronounced *dual* PPA "tracks" under the N core component; whereas only one is seen in the QN profile. The QN PPA traverse is clearly most associated with the conal emission, and RVM-fitted curves showing its PPM (green) and 90-°-shifted (magenta) traverses are overplotted. These conal RVM curves are also shown in the N and FN panels, but note that neither follows the stronger, later "diagonal" traverse that is most associated with the SPM core emission. The scale intensities of the QN and FN profiles are 99 and 103% that of the N mode profile; whereas the former has 91.4% and the latter 8.6% of the power.

gued that this was due to **secondary polarization-mode (SPM) OPM emission dominating in the core region in contrast to primary polarization-mode (PPM) emission dominating** throughout the profile otherwise.

Indeed, this N partial profile shows substantial linear depolarization under the core region that contrasts with the relatively large fractional linear polarization elsewhere. Note also that, unusually, there are *two* distinct PPA "tracks" under the core region: coincident with the linear minimum, there is a partial one (green curve) that is associated with the PPM under the conal components; and just under this curve there is a second distinct track that is centered at the PPA of the surrounding PPM emission (*i.e.,* , in the –40-70° range) and thus must represent SPM power. This second track, however, is no ordinary SPM track as we can see from the 90°-shifted PPM (magenta) curve, as it lags this curve by much of a degree! Indeed, the average (red) PPA curve follows this second track between 0 and 1° longitude. It will be interesting to see how these features will divide between the QN and FN partial profiles. Finally, note the positive-going "patch" of PPAs just prior to the longitude origin; the emission that these represent is notable because it seems not to be associated with either of the two OPMs—indeed, it appears to represent **power that is impossible to fit with any rotating vector (hereafter RVM) model. We return to consider this peculiar power below.**

Partial profiles for the QN and FN modes are given in Fig. 5 (upper and lower right, respectively). As expected, the QN profile aggregates the roughly 81% of N pulses with little to no core emission. Apart from this low level of core emission, the QN profile is almost indistinguishable from the N partial profile. Note that a small inflection can be seen in the total power corresponding to a small remaining core contribution, but hardly even a

"shadow" of "diagonal" SPM PPAs remains in the lower panel. Therefore, only here in the QN mode does the average PPA follow the **earlier** of the two "tracks" in the N profile, and the two RVM curves (green and magenta) represent joint fits to these traverses. These yield α and β values of 57.6 and –0.3°, respectively, as well as an inflection at 0° longitude and a PPA of +36.6°. The goodness of fit is largely determined by the R [$=\sin\alpha/\sin\beta$] value, and β values differing by ±0.1° or so gave acceptable fits. Interestingly, only negative values of β provided the "squarish" behaviour needed to fit this pulsar's PPA tracks. This fit is overplotted on the N, FN and Ab partial profiles.

The FN profile, by contrast, representing the remaining about 19% of the N pulses, is quite dramatic. Here we **first encounter** strong core emission, with a significant anti-symmetric V signature. The components of both cones are somewhat less linearly polarized, and overall the FN profile is slightly narrower than its QN counterpart. The core region is flanked by two linear polarization minima corresponding almost precisely to the breadth of the "diagonal" PPA feature in the lower panel. Both PPA "tracks" are clear, but the SPM one is dominant and carries most of the power noted earlier for the N profile.

The overall shape of the FN profile is worthy of note: All five components are in clear evidence, although the trailing two are slightly less resolved than the others, mostly because the outer trailing component appears earlier than in the QN profile by 0.5°. Note the "triangular" shape of the core component with its more shallow rise and steep fall-off. Note also that the deep minimum remains between the leading inner cone and core components. Here also we see very clearly the four inflections of the PPA noted in Paper I that are characteristic of the changing OPM dominance under the core component.

Finally, Figure 6 shows the 686-pulse partial profile of the abnormal (Ab) mode. Here the core is dominant with its very strong and fully anti-symmetric circularly polarized signature, the trailing components are mysteriously conflated into a single feature, and the profile overall is linearly depolarized apart from the leading inner conal feature. Also note the deep linear minimum just prior to the core, its pronounced "triangular" form and the appearance of the emission "bridge" connecting the leading inner cone and core components.

The PPA distributions also give important information: Both OPM PPA "tracks" are in evidence, but relative to the earlier profiles the SPM emission is much stronger and longer. Indeed, note that it is dominant under the surviving trailing conal component. Under the core the usual "diagonal" SPM feature is strongly in evidence, but note that there is also a second PPM PPA "track" that traces the full negative-going traverse. It starts about –1° longitude, continues clearly **through** the center of the profile, and then a weaker connection can just be discerned (beside the SPM "diagonal" feature) going all the way to the trailing PPM "track". Note

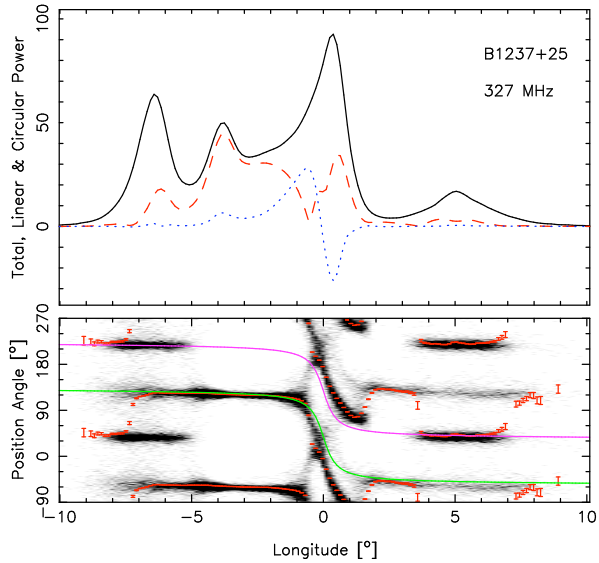

Figure 6. Partial average profile **and PPA histogram** for the abnormal (Ab) mode, after Fig. 1, comprised of 686 pulses and with a **PPA** threshold of 7°. Comparing this Ab mode profile with the N and FN partial profiles in Fig. 5, the most striking feature is the dominant core emission with its anti-symmetric circular polarization. Note also, however, the linear depolarization of the outer conal components and the appearance of the highly linearly polarized "bridge" emission that fills the region between the leading inner conal component and the core—and the deep linear minimum just prior to the core shows that the core and the "bridge" emission represent different OPMs. The scale intensities of the N and Ab profiles are 109 and 140% that of the total profile; whereas the former has 42% and the latter 58% of the overall power.

also that a weak positive-going patch of emission can also be seen just prior to the center of the profile. This patch is associated with the shallow rise of the core and the deep minimum in linear polarization.

The Ab PSs were found to exhibit their well known properties, and these distinct properties in both total power and polarization made it easy to positively identify the Ab intervals in our colour displays. This observation is unique in the number of times in which the abnormal mode occurs. Ab mode PSs appear 12 times throughout the observation. Three of these PSs were lengthy whereas the other nine were much shorter.

The separation of the observation into the three distinct modes delineated in Paper I is strongly reflected in our single pulse analysis. However, the question remains whether QN and FN intervals are actually modes or merely behaviours. The FN's core flares interrupt QN intervals fairly regularly, however, without very long N sequences, it is impossible to determine whether these interruptions occur periodically.

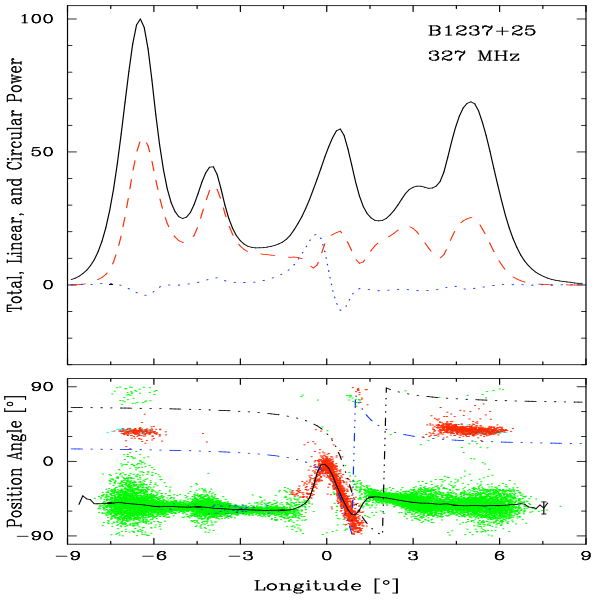

Figure 7. Flare-normal mode partial profile and OPM-segregation model after Figs. 1 and 5 (lower right). Curves indicating the OPM boundaries are given in dash-dotted blue and 'black (see text). The qualifying samples exceeding both total and linear power thresholds are shown in the lower panel. Most reflect partially polarized power and are shown in green (PPM) and red (SPM); whereas the fully polarized ones are shown in blue and cyan. The average PPA (solid black) curve follows the leading PPM power until about –1° longitude, at which point it diverts first to follow the positive-going "patch" of non-RVM power and then the strong central "diagonal" SPM traverse; whereas afterward it again diverts to follow the trailing PPM power. The SPM PPA track is incomplete because qualifying power is found only under the leading, core and trailing comps; whereas, the PPM track is so because only few such samples are found in the core region. Nonetheless, note the few that do trace the PPM track in the region just above the central "diagonal" SPM region.

5 ASSIMILATING THE PROPAGATION MODES

The splitting of core emission into the two OPMs which occurs in the Ab and FN modes seems to indicate that the core emission propagates as two independent and orthogonal EM waves. If so, then we must explore how this modal radiation is related to the O (ordinary) X (extraordinary) physical propagation modes. In our earlier work on pulsar B0329+54 (Mitra *et al.* 2007) we attempted to determine the direction of the modal PPAs with respect to the projected magnetic field by comparing the fiducial PPA and proper-motion directions, but no such line of argument is possible for this pulsar because the difference angle falls far from 0 or 90° (Johnston *et al.* 2006; Rankin 2007)—probably in part because of the pulsar's unusual position near 90° Galactic latitude.

Here we rather suggest, and assume in our further analysis, that core emission fills the polar flux tube at low altitudes and propagates outward along the magnetic axis. In order not to suffer refraction, this lower altitude core radiation must be associated with the extraordinary X physical propagation mode. This then identifies the SPM as corresponding to X-mode radiation. Some support for this suggestion seems apparent from Fig. 5 in that the SPM PPA "patches" under the outer conal comps. seem to fall slightly interior to their PPM counterparts—assuming that the two modes are emitted at similar heights, that the O mode (PPM here) is subject to refraction, and that this refraction is outward [following Barnard & Arons (1986), Lyubarskii & Petrova (1997) & Weltevrede *et al.* (2005)]. However, the overall widths in Table A1 provide a weak contrary indication.

In any case, this is the same modal identification as we made earlier for B0329+54 (Mitra *et al.* 2007).

6 ORTHOGONAL POLARIZATION MODE SEGREGATION

In few pulsars is the orthogonal polarization mode (OPM) activity more prominent that in B1237+25, as we have seen above. A major intent of this study is to look at this phenomenon more closely in an effort to glean more about the physical **circumstances** associated with OPM emission. In Paper I our conclusions were based almost entirely on partial profile analyses, here we wish to investigate the effects at the individual pulse level.

Deshpande & Rankin (2001; hereafter DR01; see Appendix) developed methods to separate PSs into polarized OPM sequences using a sample-by-sample segregation. The techniques were applied to pulsar B0329+54 (Mitra *et al.* 2007) in a manner similar to what is needed below. Thereby these authors were able to separate behaviours pertaining to a particular mode and relate them to the expected characteristics of the X and O propagation modes.

The two methods described by DR01 entail different assumptions about how the emission is depolarized: in the two-way segregation, the parent radiation is assumed to be comprised of two fully polarized OPMs that become depolarized by incoherent superposition, such that modal repolarization is feasible. By contrast, the three-way method makes no such assumption; the power is segregated into PPM, SPM and unpolarized (UP) PSs.

Each of B1237+25's emission modes (N, QN, FN and Ab) were segregated using first the two- and then the three-way methods, so that the effects of the assumptions in the former could be assessed with the latter. Results of the three-way technique are given below, whereas the two-way segregations appear in Appendix Figs. A2-A4.

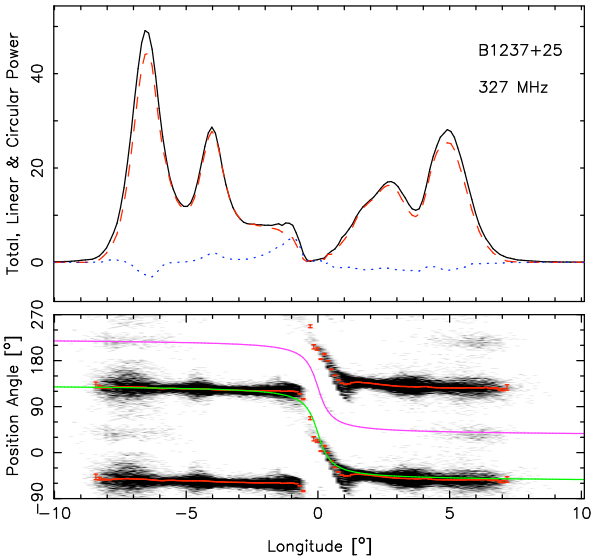

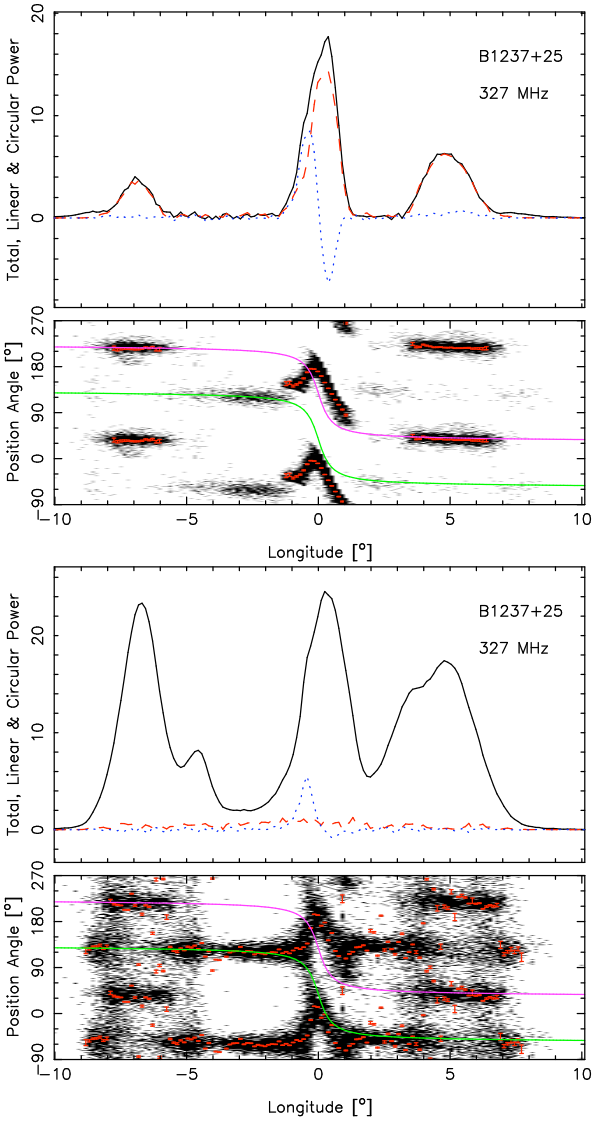

Figure 8. Flare-normal mode three-way OPM separations after Fig. 1 corresponding to the PPM (upper left), SPM (upper right) and UP (lower right) of the partial PS depicted in Fig. 5 (lower right). A threshold of 5 standard deviations in the off-pulse noise was used to build the PPM and SPM fractions, and thus they are nearly 100% linearly polarized and the UP nearly unpolarized. Similarly, only samples with PPA errors less than 5° are plotted as dots in the lower panels. The 100% intensity scales of the PPM, SPM and UP are 65, 24 and 33% that of the FN partial profile, respectively; and the three respective profiles have 51, 11 and 38% of the total power.

Because of the non-orthogonal character of the two OPMs in B1237+25's core region, this separation required significant modification of DR's techniques, and we have made most use of the three-way technique.

Both methods require a PPM PPA model which defines the ±45° modal boundaries, often provided by an RVM fit. Normally, such a model is quite forgiving as little power falls near the boundary regions. However, the OPM PPA "tracks" in B1237+25's core region are separated by hardly 40°, and care had to be taken to define the modal boundaries carefully. Our requirement here, we emphasize, is to segregate the modal power reliably, not to fit the PPA tracks precisely. RVM fits to either of this pulsar's OPMs are difficult in all respects and only confirm its highly central sightline and nearly orthogonal geometry—and our analysis depends on the exactitude of neither. We therefore discuss the four modes in turn below, beginning with the FN emission.

6.1 Flare-Normal Mode

As we saw in the bottom left panel of Fig. 5, the PPA behaviour is unusually complex in the central core region. There are two **distinct** PPA "tracks" belonging to the respective OPMs, and they are not at all orthogonal in this region. The more prominent of the two is the downward "diagonal" track centered about +0.5° longitude that must be associated with the SPM because it is centered at the same PPA as the strong regions of PPM power that precede and follow it. It traces the steep center of a negative-going PPA traverse that starts with the weak SPM "patch" under the leading conal component at +35° and ends with the similar one under the trailing component. The second PPM traverse follows the average PPA through the strong leading conal components, but there is so little PPM polarized power in parts of the central core region that the full traverse cannot be followed continuously; however, its full trajectory can be traced as described above in the panels of Fig. 5. This combined with the weak QN-mode analysis in Paper I

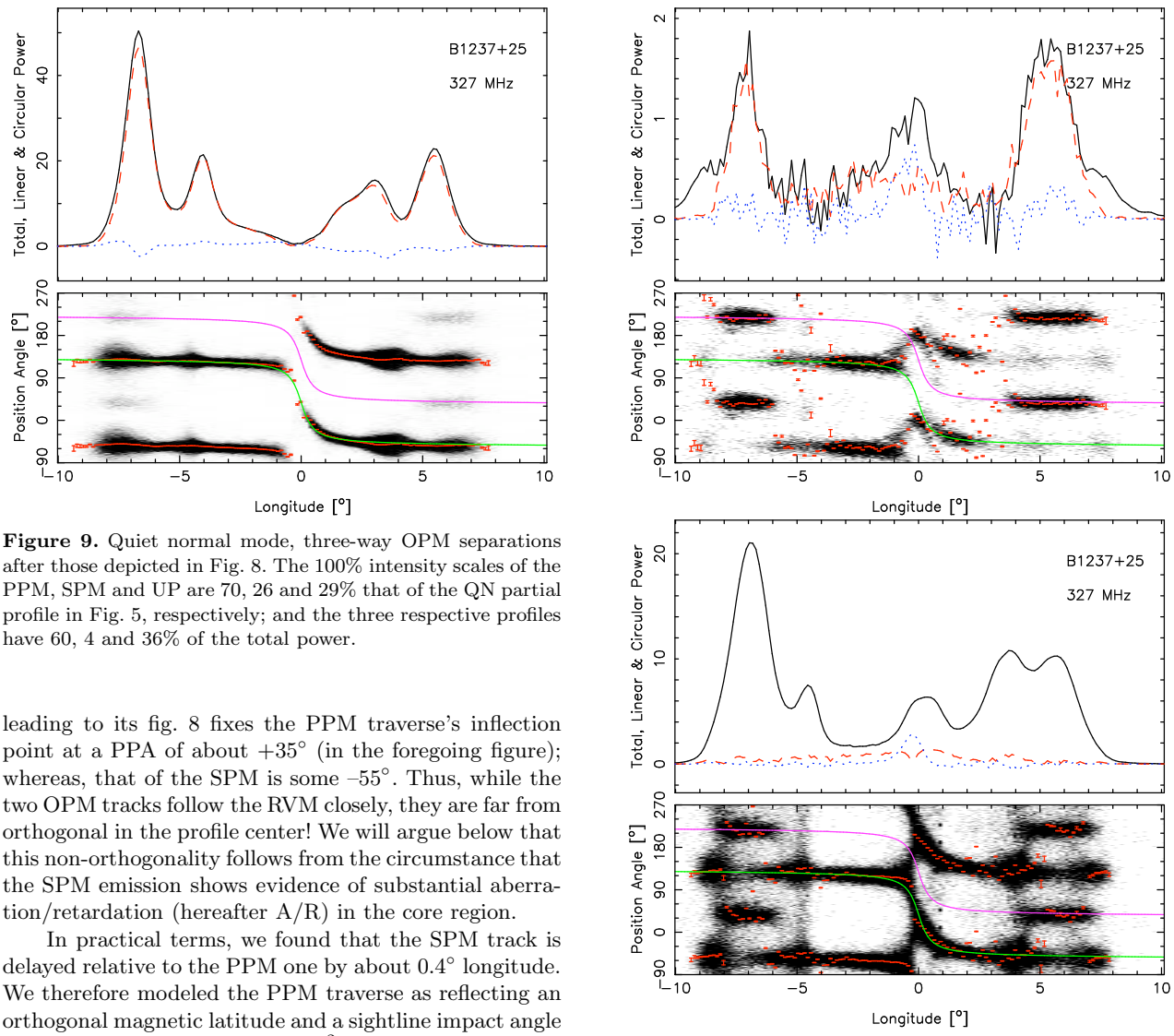

Figure 9. Quiet normal mode, three-way OPM separations after those depicted in Fig. 8. The 100% intensity scales of the PPM, SPM and UP are 70, 26 and 29% that of the QN partial profile in Fig. 5, respectively; and the three respective profiles have 60, 4 and 36% of the total power.

leading to its fig. 8 fixes the PPM traverse's inflection point at a PPA of about +35° (in the foregoing figure); whereas, that of the SPM is some –55°. Thus, while the two OPM tracks follow the RVM closely, they are far from orthogonal in the profile center! We will argue below that this non-orthogonality follows from the circumstance that the SPM emission shows evidence of substantial aberration/retardation (hereafter A/R) in the core region.

In practical terms, we found that the SPM track is delayed relative to the PPM one by about 0.4° longitude. We therefore modeled the PPM traverse as reflecting an orthogonal magnetic latitude and a sightline impact angle β of 0.5° centred at 0° longitude.[2] Then, we modeled the SPM track using the same RVM curve, but delayed by three 0.133° samples and shifted in PPA by 90°. Given the closeness of these two modal OPM-modal curves in the central region, we took the lower PPM boundary as 20° above and the upper as 30° below the model SPM PPA curve. These boundaries and the qualifying samples are shown in Figure 7 which is identical to the lower right panel of Fig. 5 apart from the colored points and curves detailing the segregated qualifying OPM points and boundaries.

Finally, note the "patch" of ostensibly positive-going (and non-RVM??) SPM samples just prior to 0°, most below the SPM boundary. This power was found to be associated with a handful of pulses having very strong SPM core emission, so we extended the boundary to include them. We will return to their interpretation below.

By the above means the FN mode partial PS was segregated into its OPM constituents, and the results are shown in Figure 8 (See also the two-way segregations in Figure A2). Only polarized power can be distinguished, however, so the three displays show the respective polarization-modal fractions: PPM and SPM (upper left and right) as well as that for the residual unpolarized power (lower right). There is much to see in these plots: First, note that both the PPM and weaker SPM profiles are fully linearly polarized out to their outside edges, and the outside half-power width of the SPM profile is slightly greater than the PPM profiles as might be expected given the latter's role in depolarizing the edges of the total profile. Note also that there is negligible SPM power under the inner conal comps. 2 and 4, although these features

[2] These values differ slightly from those obtained from the fitted curves in Fig. 5, but their effects in segregating the modes are virtually identical.

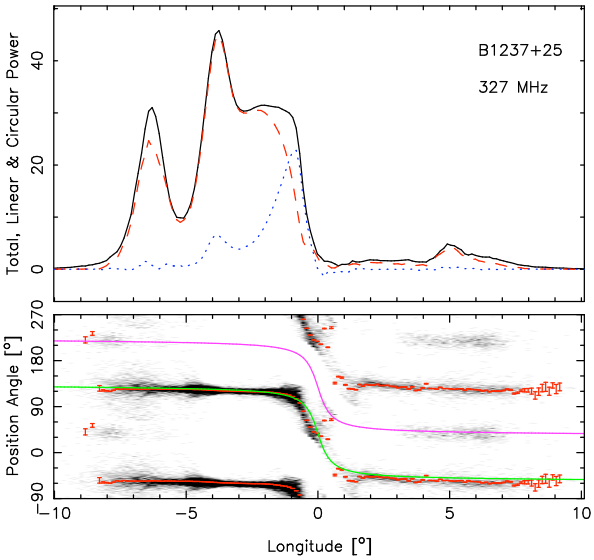

Figure 10. Abnormal mode, three-way OPM separations after those depicted in Fig. 8. The 100% intensity scales of the PPM, SPM and UP are 49, 47 and 61% that of the QN partial profile in Fig. 5, respectively; and the three respective profiles have 44, 18 and 38% of the total power.

do appear in the UP fraction—thus the PPM is always dominant here though not fully linearly polarized.

Second, of greater import here, the preponderance of the core's power is SPM emission, and this emission exhibits about equal amounts of antisymmetric (+/–; LH/RH) circular polarization. We see here again suggestions that the core has a weaker leading part in addition to its strong trailing portion—note the "triangular" or unresolved-double forms of the core feature in the SPM and UP fractions. Some of this leading-edge core power is seen in the PPM fraction about –1° longitude as well as in the SPM fraction. Also this is just the region with the ostensibly positive-going "non-RVM" SPM PPAs, and it tends to be more depolarized than adjacent regions.

6.2 Quiet Normal Mode

The three modal fractions for the QN mode are given in Figure 9 (See also the two-way segregations in Figure A3), and there are few surprises. The PPM (upper left) clearly shows the negative excursion of its PPA under the absent core component. Overall the SPM is weaker under the entire profile. Its two outer conal features seem to be a bit wider than their PPM counterparts, power is again virtually absent under the two inner conal comps., and the residual core power is just a noisy whisper in the profile center. Somewhat counter-intuitively, the UP profile is well defined—this is because nine times more power accrues to it than to the SPM profile. Finally, note that the core power in both profiles falls a bit earlier than in the FN profiles, probably because those latter tend to include most of the stronger, later core samples.

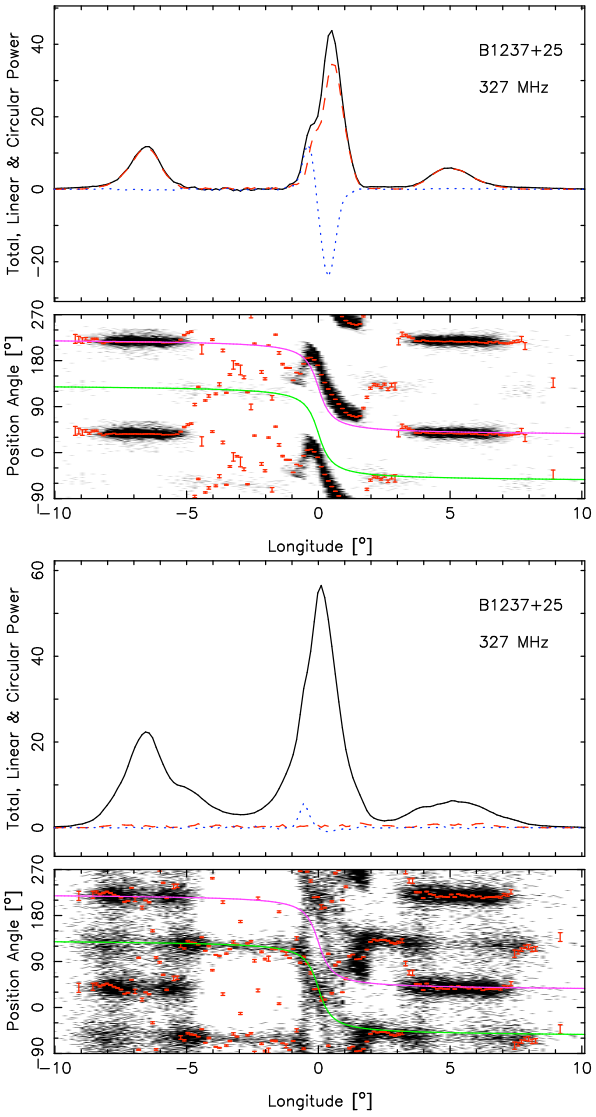

6.3 Abnormal Mode

The three-way OPM separations for the Ab mode, seen in Figure 10 (See also the two-way segregations in Figure A4) show some similaries to the behaviours seen above in the FN mode, but are much more extreme. The core dominates **its modal partial profile as can be** seen in Fig. 6 **and exhibits the same dual PPA tracks, the latter SPM one apparently indicative of A/R**. In the modal separations, the core power is divided mainly, and about equally, between the SPM and UP profiles, with some further earlier-falling PPM power in its profile. This reflects the relatively small fractional linear polarization of the Ab core (as seen earlier in its

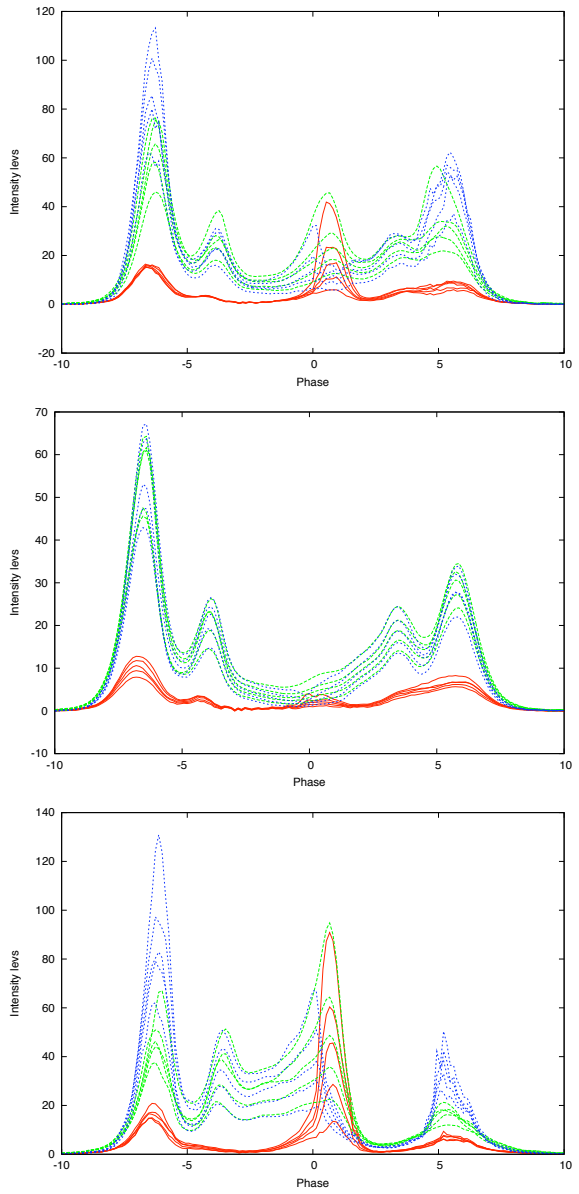

Figure 11. Intensity-fractionation analysis of the FN (top), QN (middle) and Ab (bottom). In each panel the total modal partial PS appears in blue, the PPM in green and the SPM in red. Profiles corresponding to five intensity fractions are plotted for each quantity.

FN counterpart) **resulting in part from the severe OPM depolarization**. Striking here again is the strong antisymmetric +/− Stokes V of the SPM core. Its leading edge is highly LH circularly polarized as is the trailing edge of the new PPM comp. 2 extension, and the boundary corresponds to the deep linear polarization minimum in the Ab-mode partial profile of Fig. 6. Less dramatic but almost identical effects are seen in the FN mode. Here, we can also see very clearly the unresolved double structure of the SPM core, which is a factor in its asymmetric "triangular" structure in the Ab partial profile.

Also dramatic and even mysterious is the huge change in the Ab mode's profile structure. The profile seems to go from five to four components because comps. 4 and 5 appear to merge. Less remarked on, however, is another equally profound alteration: a new "component" appears to fill in the region between comp. 2 and the core. We do not usually encounter pulsar emission components that disappear or appear, so how are we to interpret this effect? The FN SPM profile is very similar to its Ab counterpart here, only the latter is relatively about twice as strong. What is profoundly different about the B1237+25 Ab emission is the conal power distribution: here, the PPM emission in the trailing region of the profile is attenuated to almost negligible levels. And, the leading region brightens: only the comp. 2 region retains large fractional linear polarization, and the "empty" region between comp. 2 and the core fills with bright PPM emission. It is almost as if the trailing PPM emission somehow shifts to the leading side in the Ab mode.

So, at least one thing is clear: comps. 4 and 5 do not disappear. Rather, PPM emission **is greatly reduced** in the trailing regions of the Ab-mode profile, and only in the PPM mode is a delineation of comps. 4 and 5 clear. What remains then is the SPM emission, and it only has a single component in the trailing region.

7 INTENSITY FRACTIONATION OF THE POLARIZATION MODES

We used the intensity-fractionation method [*e.g.*, **see Mitra** *et al.* **(2007) for its role in the analysis of pulsar B0329+54**] to study the dynamics of the segregated profile-mode and OPM emission. Three total-power plots summarizing this analysis are given in Figure 11, but we **also referred to** corresponding sets of polarization profiles for each mode and OPM (Appendix: Figures A5 to A7). This analysis was carried out on the FN (top), QN (middle) and Ab (bottom) modes. Five levels were used such that the PS was divided into five fractions according to the intensity in the central core ($\pm 3^\circ$) region and then averaged to construct a profile.

The flare-normal (FN) mode first alerted us to the interest of this analysis. The results, summarized in the top display of Fig. 11, show how the intensity of the emission throughout the profile varies for changes in the level within the central region. First, most of the variation in this central region is associated not with the core overall (blue) but with the SPM emission (red) within it. Remarkably, the SPM conal emission varies little, nor does the PPM power in either the core or conal regions. The SPM core emission therefore appears to be an independent process. Second, the brighter the SPM core emission, the broader and more fully antisymmetrically circularly polarized it is. Finally, the SPM core emission window

appears to move earlier with larger intensity just as we had suspected above.

For contrast, we show the same analysis as applied to the QN mode in the middle panel of Fig. 11. Here we see only very weak variations in the central region as expected as well as small unsystematic variations in the OPM emission of the conal components. This is the mode in which the 2.7-P_1 periodicity most prominently modulates the conal components.

It is for the abnormal (Ab) mode, however, that intensity fractionation is most revealing (bottom panel of Fig. 11). We can see clearly here how the very different SPM and PPM contributions join together to produce the core. The SPM, though, has the larger role, and that its emission moves earlier with larger intensity **(while its PPA track shifts later, see Fig. A7)** could not be clearer here. The earlier PPM part of the core emission is strange, as it spills over all the way to the leading inner cone component—a profile region that is relatively empty of emission in the other modes. This configuration almost suggests that the SPM core has a role in exciting the PPM core emission.

This "bridge" between the second and core components is strongest by far in the Ab-mode PPM and is heavily correlated with the SPM core intensity. However, the shape of the "bridge" remains the same at all intensity levels, which indicates a continuous and secondary emission process; see Fig. A7.

Finally, the lower panels of Fig. 11 provide a convenient means of comparing the forms of the QN and Ab modal profiles. Obviously, the outer conal (outside, half-power) width of the Ab profile is somewhat narrower. We can see that the PPM width of the outer conal components is narrower than the SPM width. The remaining major mystery is what happens to the inner conal emission. Note that even in the FN profile comp. 4 has lost some of its identity, but it is hardly absent! There is little to the FN core apart from its SPM emission, but in the Ab situation, it is almost as if the entire inner cone has been shrunk and thrown forward, so that the former comp. 4 becomes the "excited" early portion of the Ab core.

8 CORE EMISSION DYNAMICS

The sequencing of modal changes has often been studied in an effort to decipher the physical processes behind them. In the present case short FN intervals seem to occur *quasi*periodically every 40-80 or so rotations with QN intervals between them. Ab apparitions can be long or short, and close inspection of the sequences suggests that such Ab intervals may start and end with FN ones. The irregular or weak core activity and 2.7-P_1 conal modulation characteristic of the FN mode seem to function as a transition to the Ab mode wherein core activity is constant and the conal modulation vanishes. FN intervals are always short, less then 20 pulses, and most "fizzle" back to QN conditions. Most Ab intervals are also short, some are clearly identifiable in only 2-3 pulses, so it is unusual for the Ab mode to "get stuck" and persist for 100-200 pulses. Similarly, Ab intervals often seem to decay into short FN sequences.

Obviously, the presence of core emission changes the dynamics of this pulsar. In the QN mode, the near absence of core emission appears to permit the formation of the fairly regularly spaced conal beamlets responsible for its long (50-60 pulse) intervals of phase-locked drifting subpulses in the outer and inner cones (*e.g.,* Hankins & Wright 1980). In FN-mode episodes, the core of course is much brighter and the regular conal modulation persists; however, these episodes are shorter (5-15 pulses), and the core action is discontinuous with even the suggestion that it too is modulated at around the conal 2.7-P_1 period. The SPM profile is slightly **wider** as can be seen in Fig. 8 and Table A1, with the shrinkage somewhat greater in the trailing two components. A close comparison of the QN and FN profiles in the figure and tables reveal as much as 0.8° shift in comps. 4/5, but only about 0.2° or less in comps. 1/2. (There is a differential shift in the OPM power.) Note also that the FN profile is more nearly symmetric—that is, its comp. 5 is stronger; however, its fractional linear is no larger, implying a larger contribution of SPM power under it. Finally, all the N-mode profiles have a broad low intensity region between comps. 2 & 3, which is conspicuous as the most highly linearly polarized (nearly complete) region in the profile. High fractional linear implies that the emission is nearly unimodal, and indeed both the 2- and 3-way OPM segregations are relatively "empty" of SPM emission here as well as in the inner cone regions of comps. 2 & 4.

The star's drama, of course, is in its Ab mode where the core is not so much brighter as more consistent. It then dominates the Ab partial profile in Fig. 6 and develops a strong and balanced antisymmetric circular polarization signature. Its form, however, is canted with a slower rise than fall, apparently due to the complex admixture of its PPM and SPM portions (see Fig. 10) and the A/R-ed SPM power (Fig. 11, bottom panel). Both OPMs importantly configure the core's power, and their respective dominance changes sharply at the deep L minimum in the above Ab partial profile at longitude –0.5°.

Most perplexing have been the conal regions of the star's Ab profile, which even seem to change from 4 to 3 components. The 2.7-P_1 modulation in the conal region vanishes entirely in Ab intervals. Ab PSs can be short (some 10 pulses), but they can also persist for well over 100 pulses, during which they are punctuated by occasional nulls—thus some are well long enough to investigate for modulation. Again, the leading conal region is less transformed that the latter; comps. 1/2 retain their positions but their is more SPM power under the leading component. In the trailing region, by contrast, comp. 4 simply vanishes, in large part because the PPM power

overall is greatly diminished, and the SPM profile narrows sufficiently on the trailing side that some workers have imagined the trailing feature to be a new component (see Fig. 10). The most puzzling feature, however, is the new power that fills in the formerly "empty" region between comp. 2 and the core. The Ab emission here is so strong that it is tempting to regard it as a "new" component, but such features are virtually unknown among pulsar profiles. Inspection of the PSs shows few peaks in this region, but rather a bright "filling in" between the two components. Note also that this emission is nearly unimodal PPM radiation—such that it is almost as if the PPM radiation in the trailing portion of the Ab PSs was redirected to this earlier region (though we hasten to emphasize that we cannot imagine how this could be physically possible!).

The intensity-fractionated diagrams in Fig. 11 permit us to estimate the extent of the A/R quantitatively. Careful measurements of them show that in both the FN and Ab modes, the brightest SPM core emission arrives about 0.21±0.03° earlier than the weakest. This value is somewhat smaller than the 3-sample, 0.40° needed shift in the SPM model PPA traverse depicted in Fig. 7, thus it appears to be underestimated by this means. It is important to reemphasize that we see this effect in only a single OPM. The above 0.40° interval corresponds to 1.5±0.5 msec, or a height difference of about 230±80 km. If we interpret this effect as we did for pulsar B0329+54 (Mitra *et al.* 2007), then we are seeing evidence of a cascade or linear amplifying process along the magnetic axis.

Finally, Paper I noted that the width of B1237+25's core component appears somewhat narrower than that expected according to the angular width of the polar cap 2.61° [$= 2.45^\circ P_1^{-1/2}/\sin\alpha$]. Given the weakness of the core in the N modes, we might expect to see the fullest development of the core in the Ab mode, where the balanced antisymmetric V is also present. The measurements in Table A1 for this core are about 2.0°—still fully half a degree short of the expected value—but both are problematic. The shape of the core feature in Fig. 6 is oddly shaped for two reasons: first, it is canted earlier due to A/R and second, the separated OPMs in Fig. A4 reveal that the PPM power in the early part of the core is significantly weaker than the SPM intensity in the trailing core. Thus we might try to estimate the full width of the core/polar cap by taking the interval between the core's SPM trailing half power point and the profile center (the zero-crossing point of the antisymmetric V) and augmenting this by the 0.40° of A/R determined above. Double this value gives a more satisfactory 2.66°.

9 SUMMARY OF THE ANALYSIS

Pulsar B1237+25's full core/double-cone geometry, relative brightness and highly central sightline traverse provide a rare opportunity to analyze and interpret its emission properties in unusual detail. In Paper I our emphasis was on examining its modal profiles; whereas, here we have been able to study the OPM properties and dynamics of its modal PSs.

Summarizing the pulsar's basic properties then from both papers—

- The pulsar has both a "normal" (N) and an "abnormal" (Ab) mode, wherein the core is relative weak/episodic and dominant, respectively. Within the former there are two contrasting core-region "quiet-" (QN) and "flare-" (FN) normal behaviours.
- Both the inner and outer conal component pairs are prominent in the N mode, exhibit the expected angular dimensions, and are modulated at an approximately 2.7-P_1 P_3 such that the beamlets (or subpulses) within the inner and outer cones are phase-locked with each other.
- The inner conal component pair is comprised largely of PPM emission as is much of the outer pair, though the exterior parts exhibit the usual effects in which their outer edges are strongly depolarized by SPM emission.
- In the Ab mode the conal modulation vanishes, PPM power in the trailing conal components (4/5) decreases sharply, core emission becomes nearly constant, and "new" bright PPM emission fills the region between the leading inner conal comp. (2) and the core region.
- the core emission is comprised of both PPM and SPM constituents, such that the very steep expected average PPA traverse is disrupted, depolarized, and exhibits the resulting (and unusual) four PPA inflections.
- The QN, FN and Ab profiles have outer conal dimensions that become progressively slightly smaller.
- The star's cone and core null together in general, up to about 5% of the time; however, the nulls in the N mode are about twice as frequent as those in the Ab mode. The N-mode nulls can persist for up to 5-6 pulses, whereas those in Ab PSs are rarely longer than a single period.
- **Nulling connects the core and conal emission: weak "sputtering" is observed during both types of nulls and suggests they are *pseudo*nulls; whereas the core involvement seems to indicate that the nulls represent cessations.**

In the analysis above we have found or clarified the following properties—

- *Geometry:* Pulsar B1237+25 provides a canonical example of core/double cone emission-beam structure, wherein our sightline cuts both cones obliquely and passes well within 1° of the magnetic axis in the core region.
- *Carousel Action:* The regular 2.7-P_1 N-mode conal periodicity is primarily stationary amplitude modulation as expected from an oblique sightline geometry and thus seems to represent orderly rotating subbeam-carousel action in a pulsar that is very far from having an aligned geometry. Other pulsars with regular drifting subpulses (*e.g.,* B0943+10 in DR) have closely aligned geometries.

B1237+25, then, seems to indicate that orderly carousel action can occur in stars with more oblique geometries.

• *Propagation Modes:* **We associate the main SPM portion of the core with the X propagation mode (as we did earlier for pulsar B0329+54). The PPM radiation is then O-mode radiation and subject to refraction.**

• *Conal Disruption by the Core?* Higher levels of core activity in this and other pulsars seem to disrupt the regular modulation in the cone. Here, the 2.7-P_1 modulation seen strongly in the QN mode and also in the FN is absent in the Ab mode—that is, **where the core emission is much more continuous**. Also, the relatively symmetric inner and outer conal emission of the N mode is highly leading-side asymmetric in the Ab mode. **Quenching of carousel action in the Ab mode appears to suppress conal emission in comps. 4/5.**

• *Aberration/Retardation:* The trailing SPM (X) portion of the core exhibits strong intensity-dependent and 0.40°-delayed-PPA A/R, such that the most intense core subpulses are dominated by the SPM and arrive earlier by at least 0.21° in the FN and Ab, respectively—amounting to about a height difference range of some 250 km. **This result is compatible with both our own earlier work on B0329+54 (Mitra *et al.* 2007) as well that of both Krishnamohan & Downs (1983) and McKinnon & Hankins (1993).**

• *Core Structure:* Both OPMs contribute to core total power over most of its width; but in very different proportions. The leading portion of the core is marked by weaker PPM (O) power and the latter by strong A/R-ed SPM (X) emission. Both the FN and Ab partial profiles show L minima at about –0.5° longitude, a point nearly coinciding with the Stokes V LHC maximum. Curiously, the antisymmetric Stokes V power is balanced despite the very different levels and dynamics of the respective PPM and SPM emission.

• *Abnormal Profile Structure:* The Ab profile is reduced to 4 components because PPM power **is greatly reduced in the trailing part of the profile—due probably to a failure of carousel action—causing** the trailing inner cone comp. (4) to vanish. Though in most regions of the profile SPM power is more prominent in the Ab mode, PPM power increases dramatically in the regions between the leading inner conal comp. (2) and the core.

• *Abnormal "Bridge" Structure:* The Ab PPM "bridge" emission between the leading inner conal comp. (2) and the core is highly correlated with the intensity-dependent A/R-ed SPM part of the core emission. The correlation is so strong as to suggest that the core has a role in producing this "bridge" emission. Moreover, the "bridge" emission's linear polarization is essentially unimodal, suggesting that it is produced at high altitude above the polarization limiting region.

10 DISCUSSION

A major concern of this paper is to shed light on the characteristics of the core emission. Core emission is not well understood. While it is often the dominant source of radiation in a pulsar's emission-beam system and seems to be ever more important for faster pulsars, it has so far been treated by no credible theory.

In B1237+25 the core exhibits three different behaviours, inactivity in the QN mode, irregular activity in the FN mode and constancy leading to dominance in the Ab mode. The core-inactive QN mode is readily understood as freeing the star to exhibit the usual properties of conal emission, drifting (in B1237+25's geometry, stationary periodic modulation), moding and nulling. Increasingly we have become accustomed to visualize the conal phenomena in terms of a rotating subbeam carousel. However, no such model has been successfully identified for this star so far—that is, we have found no means to determine the carousel circulation time (CT) or its beamlet structure. Maan & Deshpande (2008) mention that they found indications of a CT, but few details are yet given. In any case, it seems probable that FN intervals so regularly interrupt the QN that any traces of a CT are obliterated.

The brief, quasi-periodic episodes of FN mode appear to disrupt the conal order only moderately. However, they seem to bracket apparitions of the abnormal mode and may have a role in exciting it. Moderately strong, irregular core emission is a defining property of the FN behaviour, and one of the key results of this analysis is its intensity-dependent SPM aberration-retardation (A/R). This is seen both in the manner that the total power is retarded and the PPA traverse delayed by some 0.40°.

Even stronger core emission, of course, is characteristic of the abnormal mode, and we determined that it is comprised of early weaker PPM and later stronger SPM radiation, and also that **the latter** exhibits a nearly identical intensity-dependent A/R. This at least twice stronger core radiation **appears to inhibit carousel action, enhancing** the leading conal PPM emission at the expense of that in the trailing region, and **filling the** region between comp. 2 and the core with PPM emission that is highly intensity-correlated with the core. How can this be?

In a previous analysis of pulsar B0329+54 (Mitra *et al.* 2007), we identified a similar A/R phenomenon associated primarily with the X-mode core emission of this pulsar, and we interpreted the effect as linear accelerator or maser amplifier operating along the magnetic axis within the polar flux tube. And in that pulsar we also noted a "pedestal" of (primarily O-mode) emission just leading the core. Thus, in both pulsars the "pedestal" or comp.2-to-core emission—is associated primarily with the O mode and exhibits an intensity dependence. The two cores themselves, however, are both mixed mode, but

the A/R is stronger in B0329+54's X mode and apparently in B1237+25's X mode as well. How can this be?

Pulsar B1237+25's sightline traverse provides an unusually close view of its emission close to the magnetic axis. In generating the core emission, the pulsar's "engine" seems to produce X-mode (SPM) radiation at relatively low (∼1-200 km) altitudes in a cascade or linear-amplifier manner such that higher intensities come from greater heights. This parent X-mode radiation then seems to undergo conversion to the O mode in a leading region of polar fluxtube plasma, such that the conversion is nearly complete on the leading side and negligible on the other. Its antisymmetric circular polarization also may be generated in this conversion. This leading-edge, O-mode core radiation is generated/converted at high altitude, seemingly above the polarization limiting height, thus its unimodal character. Moreover, it is subject to forward refraction, such that both effects retard its phase. At the highest intensities a combination of refraction and A/R thus result in some radiation filling the region between the inner conal comp. (2) and the core. If the two effects were comparable in "spilling" O-mode radiation into the usually empty profile region about -2.5° prior to the magnetic axis, an altitude of some 1500 km would be indicated.

ACKNOWLEDGMENTS

Much of the work was made possible by support from the US National Science Foundation grants 08-07691 and 09-68296. One of us (JMR) also thanks the Anton Pannekoek Astronomical Institute of the University of Amsterdam for their generous hospitality and both Netherlands National Science Foundation and ASTRON for their visitor grants. Arecibo Observatory is operated by SRI International under a cooperative agreement with the National Science Foundation, and in alliance with Ana G. Méndez-Universidad Metropolitana, and the Universities Space Research Association. This work made use of the NASA ADS astronomical data system.

REFERENCES

Allan,M. C., & Melrose, D. B. 1982, Proc. Aston. Soc. Australia, 4, 365
Arons, J. & Barnard, J. J. 1986, *Ap.J.*, 302, 120
Backer, D.C. 1970a, Nature, 228, 42
Backer, D.C. 1970b, Nature, 228, 752
Backer, D.C. 1970c, Nature, 228, 1297
Backer, D. C. 1973 *Ap.J.*, 182, 245
Barnard, J. J. & Arons, J. 1986, *Ap.J.*, 302, 138
Bartel, N., Morris, D., Sieber, W., Hankins, T.H. 1982, *Ap.J.*, 258, 776 (BMSH)
Deshpande, A.A. & Rankin, J.M. 1999, *Ap.J.*, 524, 1008
Deshpande, A.A., Rankin, J.M., 2001, *MNRAS*, 322, 438
Hankins, T.H., & Wright, G.A.E. 1980, *Nature*, 288, 681
Herfindal, J. L., & Rankin, J. M., 2007, *MNRAS*, 380, 430
Herfindal, J. L., & Rankin, J. M., 2009, *MNRAS*, 393, 1391
Janssen G.H., van Leeuwen A.G.L. 2004, A&A, 425, 255
Johnston, S., Hobbs, G., Vigeland, S., Kramer, M., Weisberg, J. M., & Lyne, A. G. 2006, *MNRAS*, 364, 1397
Kramer, M., Lyne, A. G., OBrien, J. T., Jordan, C. A., & Lorimer, D. R. 2006, *Science*, 312, 549
Krishnamohan, S., & Downs, G. S. 1983, *Ap.J.*, 265, 372.
Lyubarsky, Y. E. 2002, astro-ph/0208566v1
Maan, Y., & Deshpande, A. A. 2008, "40 YEARS OF PULSARS: Millisecond Pulsars, Magnetars and More" AIP Conference Proceedings, 983, 103
McKinnon, M. M., & Hankins, T. H. 1993, *A&A*, 269, 325 (MH93).
Melrose, D. B. 1979, Australian J. Phys., 32, 61
Mitra, D., Rankin, J. M., & Gupta, Y. 2007, *MNRAS*, 379, 932
Petrova, S.A. 2001, A&A, 378, 883
Petrova, S.A. 2001, *MNRAS*, 324, 931
Radhakrishnan, V., & Rankin J.M., 1990, *Ap.J.*, 352, 258
Rankin J.M., 1986, *Ap.J.*, 301, 901 (ET III)
Rankin, J. M. 1993a, *Ap.J.*, 405, 285 (ET VIa)
Rankin, J. M. 1993b, *Ap.J. Suppl.*, 85, 145 (ET VIb)
Rankin, J.M., 2007, *Ap.J.*, 664, 443
Rankin, J.M., Ramachandran, R. 2003, *Ap.J.*, 590, 411 (ET VII)
Redman, S. R., Wright, G.A.E., & Rankin, J. M., 2005, *MNRAS*, 357, 859
Redman, S. R., & Rankin, J. M., 2009, *MNRAS*, 395, 1529
Srostlik Z., Rankin J.M., 2005, *MNRAS*, 362, 1121
Weltevrede, P., Edwards, R. T., & Stappers, B. W. 2006, *A&A*, 445, 243
Weltevrede, P., Stappers, B. W., van den Horn, L. J., & Edwards, R. T. 2003, *A&A*, 412, 473
Weltevrede, P., Stappers, B. W., & Edwards, R. T. 2007, *A&A*, 469, 607

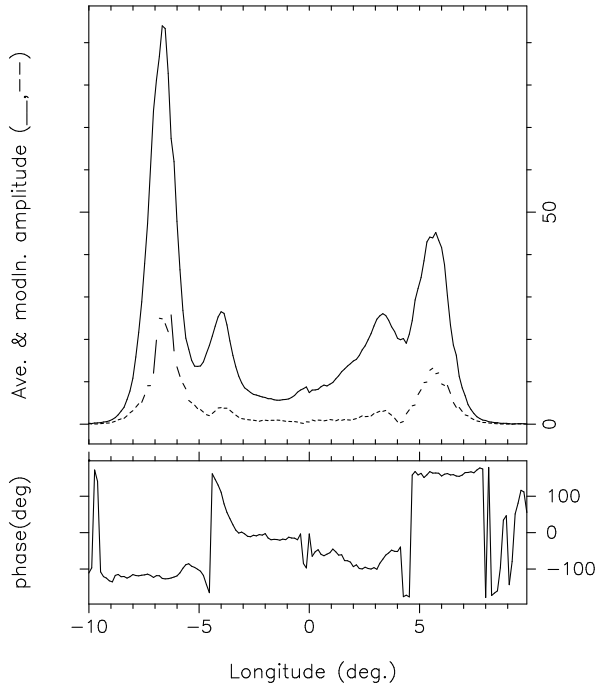

Figure A1. Modulation phase for a particularly coherent section of the QN mode (lower panel), and the total power profile and modulated power (upper panel). In this diagram only PPM power is used. A similar analysis using total power showed a significant phase slope under the outer components.

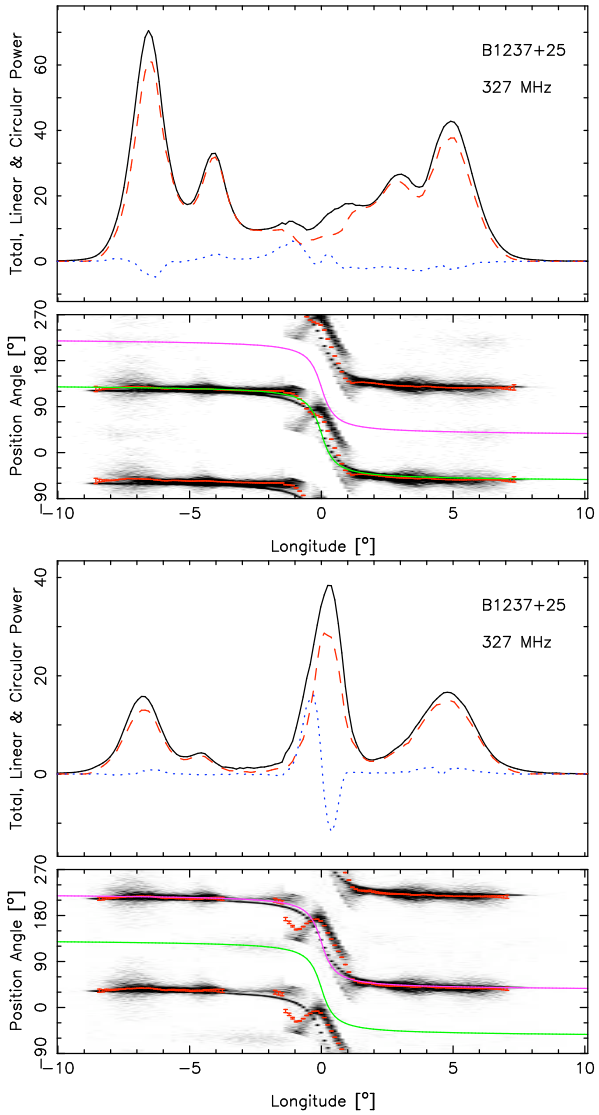

Figure A2. Flare-normal mode two-way separation, corresponding to Fig. 8 above. The 100% intensity scales of the PPM and SPM are 94 and 52% that of the FN partial profile in Fig. 5, respectively; and the respective profiles have 71 and 29% of the total power.

APPENDIX A: APPENDIX

A1 Profile measurements

Measurements of the overall half-power widths, component widths and component positions are given in Tables A1-A2. The values are of course most accurate when a particular component is relatively isolated. When not, we took the opportunity to accurately measure and then double the "freer" half of the component, of course reporting it with a larger error. When neither "edge" of a component was accessible, we estimated the position and width and marked the value with a larger error or as an approximation.

A2 Phase Modulation, not Drifting Subpulses

In their extensive fluctuation-spectral analyses using their two-dimensional Fourier-transform technique Weltevrede *et al.* (2006, 2007) came to the conclusion that B1237+25 showed "drifting in opposite directions" under its two outer conal components. Clearly, this is a strange result given the oblique manner in which the sightline cuts these components, so it is interesting to understand how these authors could have come to this conclusion. Of course, we cannot know what mode the pulsar was in when their observations were taken, but probably it was a mixed-mode PS. mostly N with a little Ab. In any case, we chose a QN interval with a particularly coherent 2.7-P_1 modulation and analysed it in two ways. We first computed a display of the modulation phase such as that in Figure A1 using the total power, and indeed it did show substantial phase ramps under the outer conal components. Then we computed the diagram above using the two-way PPM sequence, and this is the analysis in the figure. We then conclude that what the above authors saw was a polarization effect. Indeed, the OPM beamlets are offset in magnetic longitude as they rotate through the sightline, so some phase offset is expected (ET VII).

Table A1. 327-MHz Component Widths

Profile // Components	Leading Outer (°)	Leading Inner (°)	Core (°)	Trailing Inner (°)	Trailing Outer (°)	Overall Profile (°)
Total	1.46±0.03	1.56±0.10	∼2.0	≈2.5	1.96±0.10	13.73±0.07
Flare Normal	1.45±0.03	1.16±0.10	1.99±0.03	∼2.4	2.02±0.10	13.19±0.07
PPM	1.44±0.03	1.37±0.10	—	∼2.1	1.99±0.10	13.16±0.07
SPM	1.64±0.03	1.40±0.10	1.48±0.03	—	2.55±0.03	13.57±0.07
Quiet Normal	1.38±0.03	1.34±0.10	—	∼2.0	1.56±0.10	13.78±0.07
PPM	1.37±0.03	1.32±0.10	—	∼1.9	1.67±0.03	13.76±0.07
SPM	1.75±0.03	1.08±0.10	—	≈2.9	∼1.9	14.44±0.07
Abnormal	1.45±0.03	1.63±0.10	1.96±0.03	—	2.49±0.03	13.53±0.07
PPM	1.38±0.03	1.37±0.10	—	—	∼2.3	13.63±0.10
SPM	1.50±0.03	—	2.07±0.10	—	2.10±0.03	13.41±0.07

Notes: The widths of the pulsar's components are often difficult to measure when they are not fully resolved. Thus the smallest errors are for isolated components; the larger errors reflect doubling the measurement of half the width; and those values without errors are estimates.

Table A2. 327-MHz Component Positions

Profile // Components	Leading Outer (°)	Leading Inner (°)	Core (°)	Trailing Inner (°)	Trailing Outer (°)
Total	–6.58±0.05	–3.98±0.10	+0.43±0.10	+3.26±0.10	+5.40±0.10
Flare Normal	–6.45±0.05	–4.00±0.05	—	+3.2±0.2	+5.15±0.05
PPM	–6.48±0.05	-4.00±0.05	—	+3.02±0.20	+4.98±0.05
SPM	–6.70±0.05	–4.54±0.20	+0.35±0.06	—	+4.88±0.05
Quiet Normal	–6.66±0.05	–4.07±0.05	—	+3.35±0.20	+5.64±0.05
PPM	–6.69±0.05	–4.06±0.10	—	+3.22±0.2	+5.58±0.05
SPM	–6.64±0.05	–4.38±0.10	—	—	+5.70±0.10
Abnormal	–6.33±0.05	–3.73±0.10	+0.42±0.10	—	+5.1±0.2
PPM	–6.29±0.05	–3.68±0.10	—	—	+5.2±0.2
SPM	–6.88±0.05	—	+0.40±0.10	—	+5.1±0.2

A3 Two-way Segregations

The results of the two-way OPM segregations are given in Figures A2 to A4 for the FN, QN and Ab modes, respectively. Here we used the same modal boundary adjustments as depicted in Fig. 7 above, but otherwise the segregations proceeded according to the algorithm described in the Appendix of Deshpande & Rankin (2001).

A4 Three-way Intensity-Polarization Segregations

Here, we give the full polarization information for each of the three PPM, SPM and UP segregations for each of the five intensity levels of the FN mode in Figure A5, the QN mode in Figure A6, and the Ab mode in Figure A7. The model curves and other presentation is identical to that in the similar displays of the main paper.

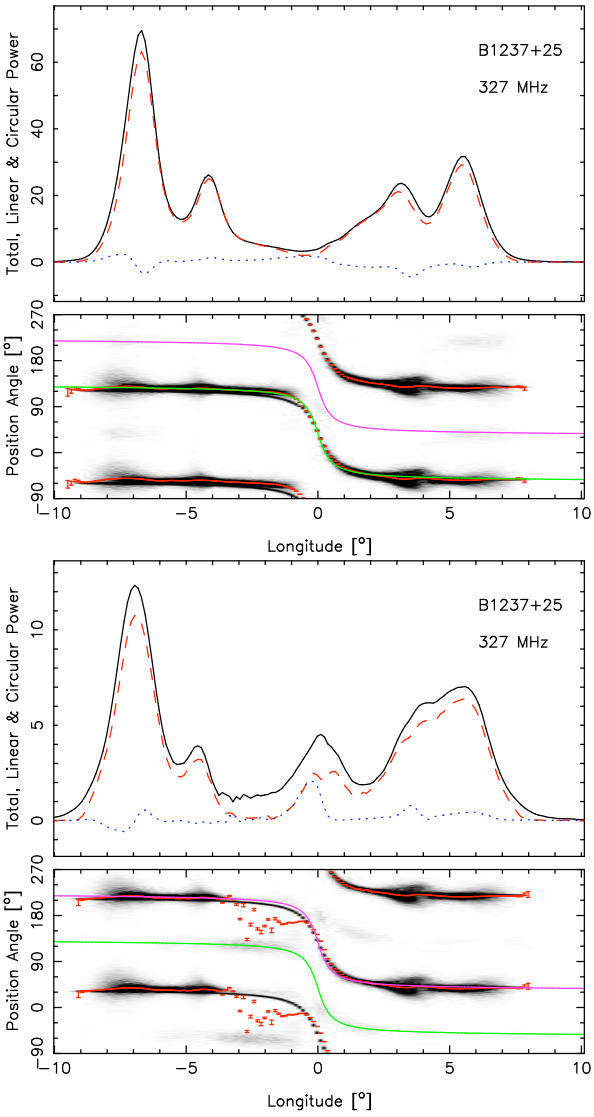

Figure A3. Quiet normal mode two-way separation, corresponding to Fig. 9 above. The 100% intensity scales of the PPM and SPM are 80 and 20% that of the QN partial profile in Fig. 5, respectively; and the respective profiles have 71 and 29% of the total power.

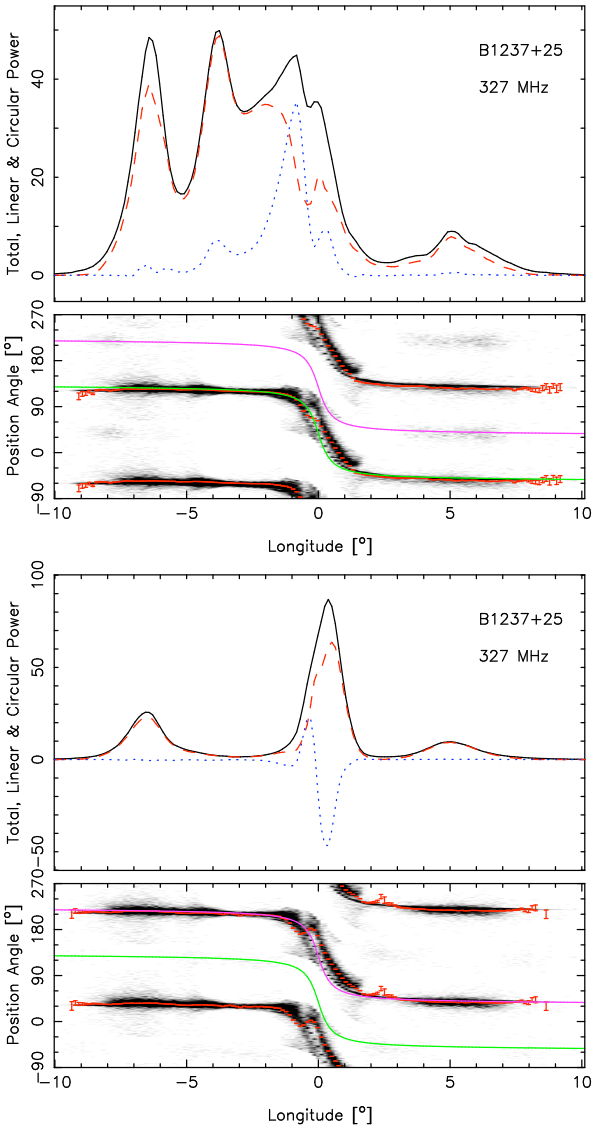

Figure A4. Quiet normal mode two-way separation, corresponding to Fig. 10 above. The 100% intensity scales of the PPM and SPM are 54 and 94% that of the Ab partial profile in Fig. 5, respectively; and the respective profiles have 61 and 39% of the total power.

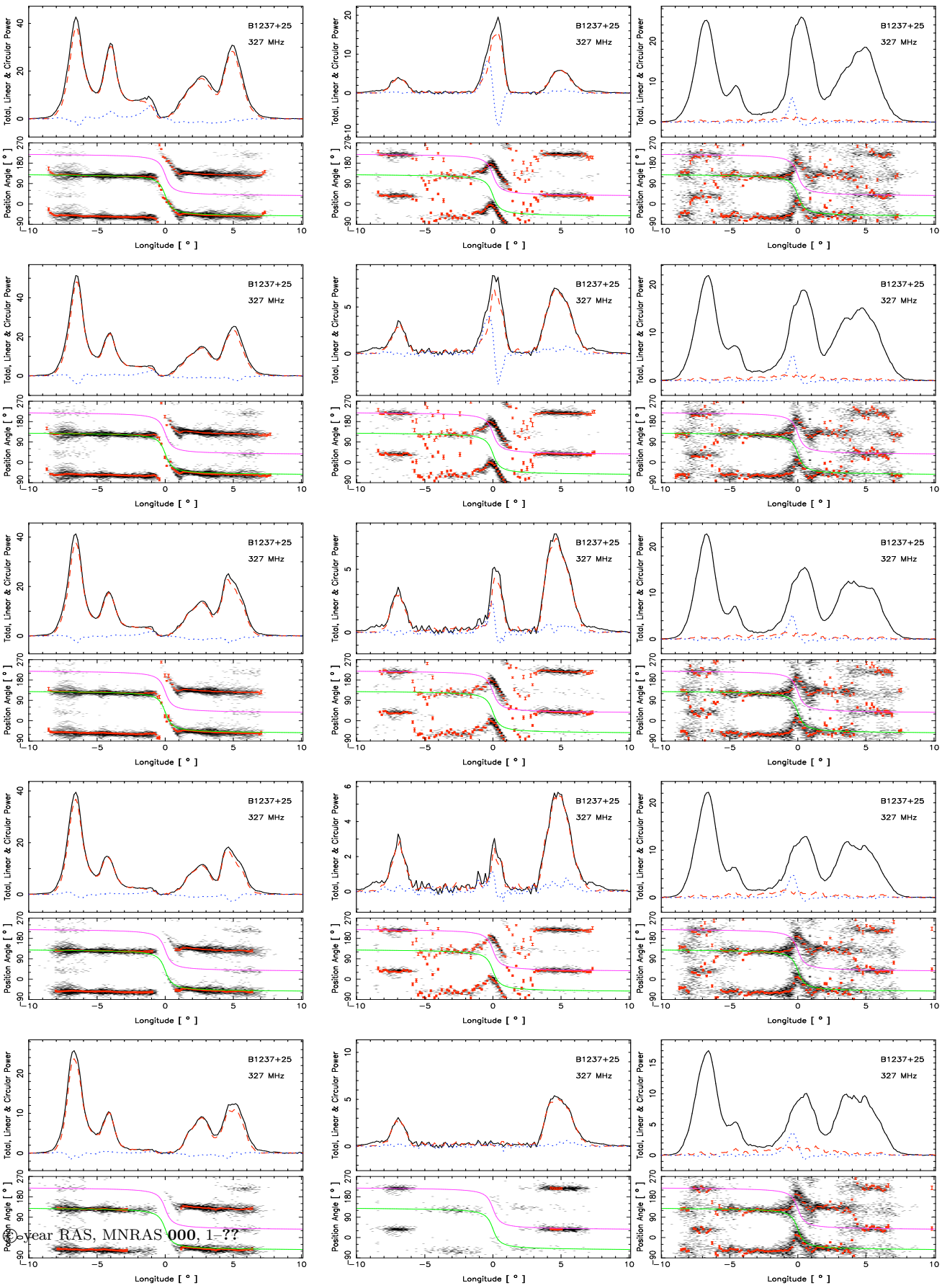

Figure A5. Flare-normal (FN) mode intensity fractions.

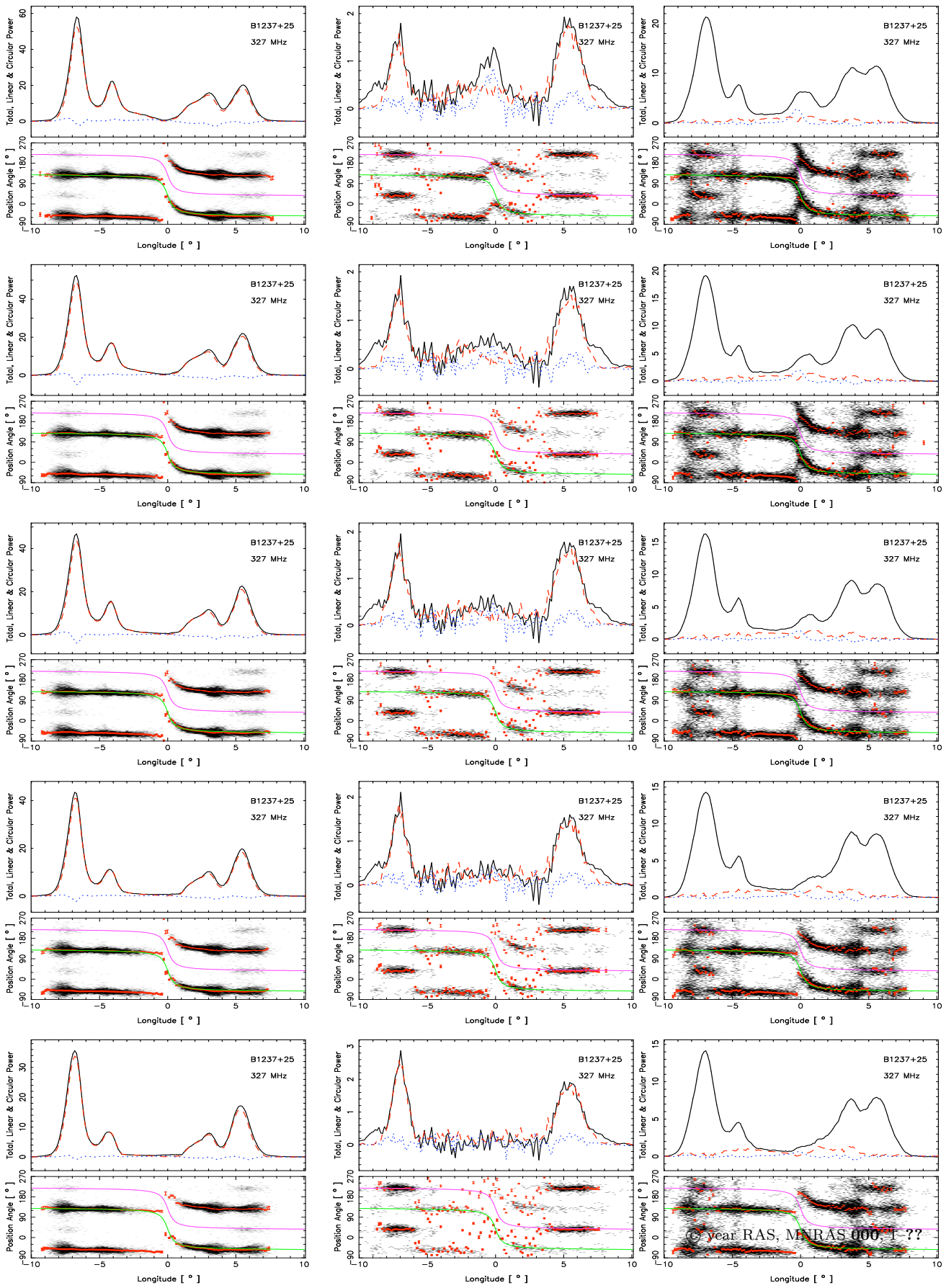

Figure A6. Quiet normal (QN) mode intensity fractions.

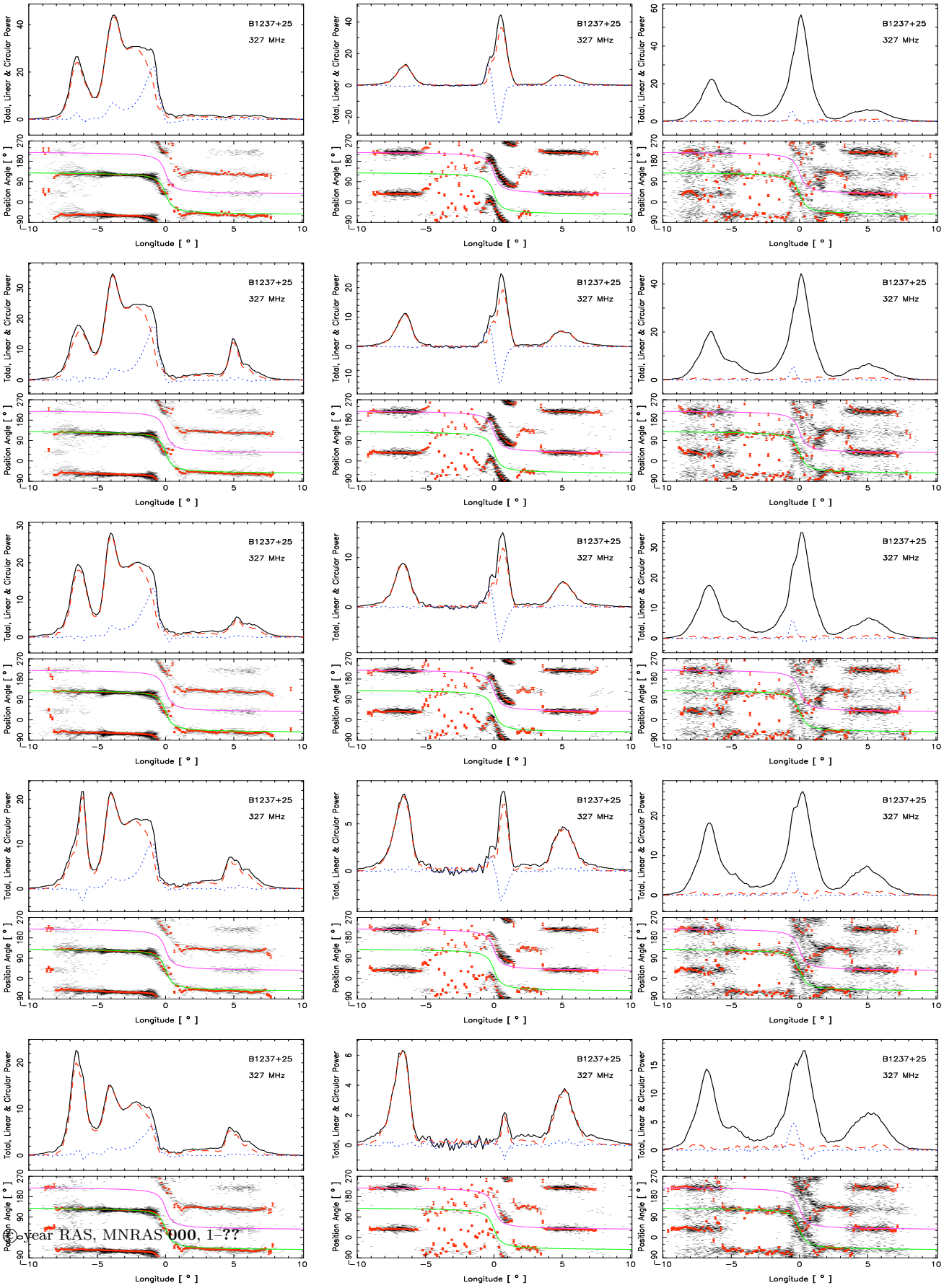

Figure A7. Abnormal (Ab) mode intensity fractions.